

Track Retrodiction for HFSWR

DRDC-RDDC-2016-P053

Zhen Ding and Peter Moo
Wide Area Surveillance Radar Group
Defence R&D Canada
Ottawa, Canada
zhen.ding@drdc-rddc.gc.ca
peter.Moo@drdc-rddc.gc.ca

Abstract—In this paper, we explore the possibility of track retrodiction to improve the track performance when a radar’s track output rate can be reduced and delayed. In the case of High Frequency Surface Wave Radar (HFSWR), the output rate may be reduced to half an hour, instead of its regular update rate of about four minutes. This allows us to accumulate seven frames of data to optimize the track output. To make use of the extra multi-frame data, we borrow the Rauch-Tung-Striebel (RTS) algorithm for the track retrodiction purpose. Using a converted extended Kalman filter (CMEKF) as the baseline, its retrodicted version, namely the retrodicted CMEKF, shows a significant improvement in performance. Monte Carlo simulation is used to verify the effectiveness of this technique. Analysis shows that the position root mean squared error (RMSE) is reduced by 30% and the RMSE in velocity is reduced by 25% when seven frame retrodiction is used. Beyond 10 frames, the reduced RMSE becomes negligible, which means that future data beyond 10 frames does not significantly improve tracking performance.

I. INTRODUCTION

High Frequency Surface Wave Radar (HFSWR) allows detection of ships beyond over the visual horizon [1]. Track update is in the order of minutes. Recently, a question, to output track data less frequently, in the order of half an hour, has been asked. It is believed that track performance can be improved with the incorporation of multiple frames of “future” data.

The question can be answered by testing a technique called *retrodiction*. Under this technique, two categories of problems and algorithms have been formulated in target tracking community. The first one, named as *track retrodiction*, is the problem of track smoothing by incorporating multiple frames of data. The other one, *association retrodiction*, is the correction of data association by possibly re-assigning multiple frames of data in a data association algorithm. The emphasis of this study is on the *track retrodiction* which assumes no modification of previous association. A recommendation is proposed to include the *association retrodiction* for further performance improvement.

Retrodiction was coined by Oliver Drummond in a series of papers [2], [3], [4]. Its definition is as follows:

The process of computing estimates of states or hypothesis probabilities for a prior time or a period of time based on data up to and including some subsequent time, typically, the present time. While prediction is the process of computing probabilities or estimates for conditions in the future, *retrodiction*

is the process of computing probabilities or estimates for conditions in the past.

According to the definition, both track retrodiction and association retrodiction can be easily understood. Both of them use “historical frames of data”, in the hope of obtaining improved performance. In fact, association retrodiction may have three sub-processes: backward association correction, forward track correction and backward track retrodiction. The processing with out-of-sequence measurements (OOSM), either update or removal with OOSM [5], [6], is an example of association retrodiction, where some OOSM are found to be associated with an existing track.

Traditionally, a radar system is always required to output its current tracks, therefore, *track retrodiction* was not as widely studied as filtering. In [7], [8], a *fixed-interval retrodiction* approach was proposed for Bayesian IMM-MHT for maneuvering targets. The approach assumes a certain time delay is tolerable, so that improved track accuracy can be achieved. On the other hand, there are strong reasons to use multiple frame data for improved data association performance [9]. It is also noted that some of the multi-frame algorithms involve the process of correcting past association decisions, and they belong to the category of *association retrodiction*. Similar terminologies are found in the literature such as *retrodicted hypotheses*, *retrodicted probability*, *retrodicted track and retrodicted estimate*, where retrodiction is considered as the antonym of “prediction” [2], [3], [4], [8].

In this study, we demonstrate that more accurate tracks can be achieved by the application of a standard Rauch-Tung-Striebel (RTS) smoothing algorithm [10] to HFSWR data. Monte Carlo simulation is used to verify the performance enhancement, based on two performance measures: filter accuracy and filter consistency. For filter accuracy, the root mean square error (RMSE) is used. For consistency, normalized estimation error squared (NEES) is used. Also compared are the effect of the number of frames to the track performance improvement.

In Section II, we summarize the radar tracking models utilized in this application and we describe the track rodition algorithm in Section III. Section IV provides the measures of performance. The results of the simulations are presented in Section V. Section VI concludes the report.

II. TRACKING MODELS OF THE HFSWR

Radar tracking requires the specification of the target state-space model and the measurement model. The discrete-time

constant velocity model is considered here as the state-space model, i.e.,

$$X(t_{k+1}) = F(T_k)X(t_k) + G(T_k)v(t_k), \quad (1)$$

where

$$X(t_k) = \begin{bmatrix} x_1(t_k) \\ x_2(t_k) \\ x_3(t_k) \\ x_4(t_k) \end{bmatrix}, \quad (2)$$

$$F(T_k) = \begin{bmatrix} 1 & T_k & 0 & 0 \\ 0 & 1 & 0 & 0 \\ 0 & 0 & 1 & T_k \\ 0 & 0 & 0 & 1 \end{bmatrix}, \quad (3)$$

$$G(T_k) = \begin{bmatrix} \frac{T_k^2}{2} & 0 \\ \frac{T_k}{2} & 0 \\ 0 & \frac{T_k^2}{2} \\ 0 & \frac{T_k}{2} \end{bmatrix}, \quad (4)$$

$$Q(t_k) = E\{v(t_k)v^T(t_k)\}, \quad (5)$$

$$= \sigma^2(t_k)I_2,$$

where $X(t_k)$ is the state vector of position and velocity along x and y directions in a Cartesian coordinate system, respectively, I_2 is a two-dimensional unit matrix and $\sigma^2(t_k)$ is the variance of the zero-mean Gaussian process noise. Also, $T_k = t_{k+1} - t_k$, and superscript T stands for the transpose of a matrix or vector.

Note that the state-space model described is for non-maneuvring and weak manoeuvring target tracking. When the targets present more complicated motion dynamics, other manoeuvring models or multiple model approach shall be considered.

The measurement model of 2-D and 3-D coherent radars is given by (a subset of) measurements of range, azimuth, elevation and Doppler. Non-coherent radars do not provide Doppler measurements. In this study, we consider the HFSWR, a 2-D coherent radar. Thus,

$$Z(t_{k+1}) = \begin{bmatrix} z_1(t_{k+1}) \\ z_2(t_{k+1}) \\ z_3(t_{k+1}) \end{bmatrix} = \begin{bmatrix} r(t_{k+1}) \\ \theta(t_{k+1}) \\ \dot{r}(t_{k+1}) \end{bmatrix}, \quad (6)$$

$$= h(X(t_{k+1})) + \begin{bmatrix} w_1(t_{k+1}) \\ w_2(t_{k+1}) \\ w_3(t_{k+1}) \end{bmatrix}, \quad (7)$$

where

$$r(t_{k+1}) = \sqrt{x_1^2(t_{k+1}) + x_3^2(t_{k+1})} + w_1(t_{k+1}), \quad (8)$$

$$\theta(t_{k+1}) = \tan^{-1} \frac{x_3(t_{k+1})}{x_1(t_{k+1})} + w_2(t_{k+1}), \quad (9)$$

$$\dot{r}(t_{k+1}) = \frac{x_1(t_{k+1})x_2(t_{k+1}) + x_3(t_{k+1})x_4(t_{k+1})}{\sqrt{x_1^2(t_{k+1}) + x_3^2(t_{k+1})}} + w_3(t_{k+1}), \quad (10)$$

and where the noise vector of $w(t_k)$ has three independent zero-mean Gaussian components. The covariance matrix $R(t_k)$

of this noise vector is as follows:

$$R(t_{k+1}) = E\{w(t_{k+1})w^T(t_{k+1})\},$$

$$= \begin{bmatrix} \sigma_r^2(t_{k+1}) & 0 & 0 \\ 0 & \sigma_\theta^2(t_{k+1}) & 0 \\ 0 & 0 & \sigma_{\dot{r}}^2(t_{k+1}) \end{bmatrix} \quad (11)$$

As shown above, the state-space model given by Equation (1) is a linear function and the measurement model given by Equations (9-10) are three nonlinear functions. Therefore, nonlinear filtering is needed for HFSWR systems.

In an HFSWR system, the range and azimuth measurements are typically converted from polar to Cartesian coordinates and a converted measurement EKF (CMEKF) is used. The measurement model for the CMEKF becomes as follows.

$$Z^c(t_{k+1}) = \begin{bmatrix} z_1^c(t_{k+1}) \\ z_2^c(t_{k+1}) \\ z_3^c(t_{k+1}) \end{bmatrix},$$

$$= h^c(X(t_{k+1})) + w^c(t_{k+1}), \quad (12)$$

where

$$z_1^c(t_{k+1}) = r(t_{k+1}) \cos(\theta(t_{k+1})), \quad (13)$$

$$z_2^c(t_{k+1}) = r(t_{k+1}) \sin(\theta(t_{k+1})), \quad (14)$$

$$z_3^c(t_{k+1}) = \dot{r}(t_{k+1}). \quad (15)$$

The covariance matrix of the converted noise vector $w^c(t_{k+1})$ is given by

$$R^c(t_{k+1}) = E\{w^c(t_{k+1})(w^c(t_{k+1}))^T\},$$

$$= \begin{bmatrix} \sigma_x^2(t_{k+1}) & \sigma_{xy}(t_{k+1}) & 0 \\ \sigma_{xy}(t_{k+1}) & \sigma_y^2(t_{k+1}) & 0 \\ 0 & 0 & \sigma_r^2(t_{k+1}) \end{bmatrix}, \quad (16)$$

where

$$\sigma_x^2(t_{k+1}) = r^2(t_{k+1})\sigma_\theta^2(t_{k+1})\sin^2(\theta(t_{k+1})) + \sigma_r^2(t_{k+1})\cos^2(\theta(t_{k+1})), \quad (17)$$

$$\sigma_y^2(t_{k+1}) = r^2(t_{k+1})\sigma_\theta^2(t_{k+1})\cos^2(\theta(t_{k+1})) + \sigma_r^2(t_{k+1})\sin^2(\theta(t_{k+1})), \quad (18)$$

$$\sigma_{xy}(t_{k+1}) = (\sigma_r^2(t_{k+1}) - r^2(t_{k+1})\sigma_\theta^2(t_{k+1})) \sin(\theta(t_{k+1}))\cos(\theta(t_{k+1})). \quad (19)$$

Note that the converted measurement covariance matrix is no longer diagonal.

III. TRACK RETRODICTION

Track retrodiction is an additional processing on top of the traditional track estimation. Typically, a retrodiction window length L is specified. During the retrodiction, all track states are "re-estimated" based the traditional track estimates and some future measurements within the selected window. In other words, two steps are involved. These two steps, the track estimation (step 1) and track retrodiction (step 2), are described in this section.

A. Step 1: track estimation

The extended Kalman filter (EKF) is the traditional and most widely used nonlinear filter in real world radar tracking systems. In this algorithm, the measurement model and/or the state-space model are linearized around the predicted state estimate.

Assume $\hat{X}(t_k)$ and $P(t_k)$ are known. At the beginning t_0 , $\hat{X}(t_0)$ and $P(t_0)$ are typically given by a track initialization approach. The EKF includes two sequential processings: prediction and update.

EKF prediction: In this step, the following three quantities are computed: state, covariance and expected state prediction.

State prediction: Propagate the state to the new measurement time t_{k+1} .

$$\hat{X}(t_{k+1|k}) = F(T_k)\hat{X}(t_k). \quad (20)$$

Covariance matrix prediction: Propagate the estimation error covariance to t_{k+1} .

$$P(t_{k+1|k}) = F(T_k)P(t_k)F^T(T_k) + G(T_k)Q(t_k)G^T(T_k). \quad (21)$$

Measurement prediction: Predict the center of future radar measurement at t_{k+1} .

$$\hat{Z}(t_{k+1|k}) = h(\hat{X}(t_k)). \quad (22)$$

EKF update: This step includes the calculation of the Kalman gain, the updates of the state and the covariance matrix.

Kalman gain update: The innovation is defined as $Z(t_{k+1}) - \hat{Z}(t_{k+1|k})$, and its covariance $S(t_{k+1})$ is given by:

$$S(t_{k+1}) = H(t_{k+1})P(t_{k+1|k})H^T(t_{k+1}) + R(t_{k+1}) \quad (23)$$

where the Jacobian matrix for HFSWR is given by

$$H(t_{k+1}) = \left. \frac{\partial h}{\partial X} \right|_{X=\hat{X}(t_{k+1|k})},$$

$$= \begin{bmatrix} \frac{x_1}{r} & 0 & \frac{x_3}{r} & 0 \\ -\frac{x_3}{r^2} & 0 & \frac{x_1}{r^2} & 0 \\ \frac{x_2x_3^2 - x_1x_3x_4}{r^3} & \frac{x_1}{r} & \frac{x_1^2x_4 - x_1x_2x_3}{r^3} & \frac{x_3}{r} \end{bmatrix}. \quad (24)$$

The EKF gain, $K(t_k)$, is a weight factor that determines the contribution of the new measurement $Z(t_{k+1})$ to the state update and it is given by

$$K(t_{k+1}) = P(t_{k+1|k})H^T(t_{k+1})S^{-1}(t_{k+1}). \quad (25)$$

State update:

$$\hat{X}(t_{k+1}) = \hat{X}(t_{k+1|k}) + K(t_{k+1})[Z(t_{k+1}) - \hat{Z}(t_{k+1|k})]. \quad (26)$$

Covariance update:

$$P(t_{k+1}) = [I - K(t_{k+1})H(t_{k+1})]P(t_{k+1|k}), \quad (27)$$

where I is a unit matrix with 4 dimensions.

The Jacobian matrix for the CMEKF is given by the following equation:

$$H^c(t_{k+1}) = \left. \frac{\partial h^c}{\partial X} \right|_{X=\hat{X}(t_{k+1|k})},$$

$$= \begin{bmatrix} 1 & 0 & 0 & 0 \\ 0 & 0 & 1 & 0 \\ \frac{x_2x_3^2 - x_1x_3x_4}{r^3} & \frac{x_1}{r} & \frac{x_1^2x_4 - x_1x_2x_3}{r^3} & \frac{x_3}{r} \end{bmatrix}. \quad (28)$$

The nonlinear filtering equations of the EKF can be used for the CMEKF. However, $Z(t_{k+1})$, $h(\cdot)$, $R(t_{k+1})$, $H(t_{k+1})$ of the EKF shall be replaced with $Z^c(t_{k+1})$, $h^c(\cdot)$, $R^c(t_{k+1})$, $H^c(t_{k+1})$ of the CMEKF, respectively.

B. Step 2: track retrodiction

Assume that $\hat{X}(t_{k+1})$ and $P(t_{k+1})$ have already been obtained from the equations in Step 1. L frames of data are used for the track retrodiction. The data includes the current frame at t_{k+1} .

The RTS algorithm uses an iterative approach to calculate track retrodiction one frame backward a time, starting from t_k [10]. Note that no extra data is available for track retrodiction at t_{k+1} . Track retrodiction is given by the following equations:

$$\hat{X}(t_{k|L}) = \hat{X}(t_k) + C(t_k)[\hat{X}(t_{k+1|L}) - F(T_k)\hat{X}(t_k)], \quad (29)$$

$$C(t_k) = P(t_k)[F(T_k)P(t_k)F^T(T_k) - G(T_k)Q(t_k)G^T(T_k)]^{-1}, \quad (30)$$

$$= P(t_k)F^T(T_k)P^{-1}(t_{k+1|k}). \quad (31)$$

The solution is in the form of a backward recursive equation that relates the re-estimation of $\hat{x}(t_k)$ given $\hat{x}(t_k + 1)$ and $Z(t_{k+1})$. Hence, the track retrodiction can be obtained from the CMEKF solutions by computing backwards using Equation (31). For easy reference, the resulted algorithm is named as the Retrodicted CMEKF in the rest of the report.

Subtract $\hat{X}(t_{k|L})$ from both sides of Equation (29) and rearranging the terms, we find

$$\tilde{X}(t_{k|L}) + C(t_k) = \tilde{X}(t_k) + C(t_k)F(T_k)\hat{X}(t_k). \quad (32)$$

Therefore, $P(t_{k|L})$ satisfies the recursive equation

$$P(t_{k|L}) = P(t_k) + C(t_k)(P(t_{k+1|L}) - P(t_{k+1|k}))C^T(t_k). \quad (33)$$

The computation is initiated by specifying $P(t_{k+1})$. This essentially completes the RTS solution for track retrodiction. It should be noted that the estimate $\hat{X}(t_k)$ are assumed to have been obtained in the process of computing $\hat{X}(t_{k+1})$ and hence can be made available by storing them in the memory. The covariance $P(t_k)$ also may be stored. However, it can be easily computed. The following formula for computing $P(t_k)$ from $P(t_{k+1})$ eliminates the extra storage for $P(t_k)$ ($k = t_0, \dots, t_k$), which is not a problem nowadays.

$$P(t_{k+1|k}) = (P^{-1}(t_{k+1}) - H^c(t_{k+1})'R^c(t_{k+1})H^c(t_{k+1})),$$

$$P(t_{k|k}) = F^{-1}(T_k)(P(t_{k+1|k}) - G(T_k)Q(t_k)G^T(T_k))(F^T)^{-1}(T_k). \quad (34)$$

IV. MEASURES OF PERFORMANCE

The measures of performance (MOPs) are used to evaluate the above track retrodiction approach. When ground truth is available, the state estimation error (EE) can be used.

The state EE $\tilde{X}(t_{k+1})$ is expressed as

$$\tilde{X}(t_{k+1}) = X(t_{k+1}) - \hat{X}(t_{k+1}), \quad (35)$$

where $X(t_{k+1})$ is the ground truth and the covariance matrix corresponding to EE is $P(t_{k+1})$ given by the track estimation or track retrodiction.

In this study, two measures of performance are used: (a) EE statistics; (b) Consistency between the EE and its covariance.

A. Measure of error statistics

The absolute errors are evaluated by the RMSE, which are calculated using the EE.

$$RMSE_{pos} = \sqrt{\frac{1}{N} \sum_{i=1}^N (\tilde{x}_{1,i}^2(t_{k+1}) + \tilde{x}_{3,i}^2(t_{k+1}))}, \quad (36)$$

$$RMSE_{vol} = \sqrt{\frac{1}{N} \sum_{i=1}^N (\tilde{x}_{2,i}^2(t_{k+1}) + \tilde{x}_{4,i}^2(t_{k+1}))}, \quad (37)$$

where $\tilde{x}_{j,i}(t_{k+1})$ is the j^{th} component of $\tilde{X}(t_{k+1})$ the i^{th} run.

B. Measure of consistency

The consistency evaluation is vital for verifying a filter design. It is done by checking the covariance matching and unbiasedness. Define the i^{th} -run normalized estimation error squared (NEES) and the N-run average NEES as

$$\epsilon_{NEES}^i(t_{k+1}) = \tilde{X}^T(t_{k+1})P^{-1}(t_{k+1})\tilde{X}(t_{k+1}) \Big|_{the\ i^{th}\ run}, \quad (38)$$

$$\bar{\epsilon}_{NEES}(t_{k+1}) = \frac{1}{N} \sum_{i=1}^N \epsilon_{NEES}^i(t_{k+1}). \quad (39)$$

The hypothesis H_0 for the filter consistency is to check whether the following equation is acceptable:

$$E[\bar{\epsilon}_{NEES}(t_{k+1})] = n_x, \quad (40)$$

where n_x is the dimension of the state X . Since $N\bar{\epsilon}_{NEES}(t_{k+1})$ has a χ -square density with Nn_x degrees of freedom. Then, hypothesis H_0 is acceptable if

$$\bar{\epsilon}_{NEES}(t_{k+1}) \in [r_1, r_2], \quad (41)$$

where the acceptance interval is determined such that

$$P\{\bar{\epsilon}_{NEES}(t_{k+1}) \in [r_1, r_2] | H_0\} = 1 - \alpha. \quad (42)$$

The interval values can be obtained from a χ -square table or calculated from the distribution calculator ‘‘DistCalc’’ by H. Lohninger of Vienna University of Technology, which is what was used. For example, for our simulations runs, $N = 1000$, $n_x = 4$, the two-sided interval is, $r_1 = 3.81$ and $r_2 = 4.2$, which gives 95% confidence to accept the hypothesis H_0 .

V. MONTE CARLO SIMULATION RESULTS

Results obtained on Monte Carlo simulation are presented in this section. The simulations were carried out to test the performance of the algorithms over 1000 Monte Carlo runs. The two algorithms, the CMEKF and the Retrodicted CMEKF with various lengths, are compared. The parameters are presented in Table I. They are based on parameters of real HFSWR. The simulations are characterized by a small process noise that captures typical non-maneuvering trajectories.

TABLE I. SIMULATION PARAMETERS

Parameter	HFSWR
Process noise (q)	10^{-3}
Range standard deviation (σ_r , m)	1200
Azimuth standard deviation (σ_θ , degree)	0.65
Range rate standard deviation (σ_r , m/s)	0.5
Measurement time interval (ΔT , sec)	262
Number of measurements	50
Initial position $[x, y]$ (m)	$[1.65 \times 10^5, 1.65 \times 10^5]$
Initial velocity $[v_x, v_y]$ (m/sec)	[5, 5]

Figures 1 and 2 show that the RMSE in position and velocity obtained in the simulations for each algorithm. It is noted that the performance of the Retrodicted CMEKF is significantly better. Figure 3 shows the normalized estimation error squared (NEES) metric for the simulations. It shows both algorithms provided consistent state estimation. In Figures 1 to 3, the retrodiction length $L = 7$ was used. The trend of the error reduction seems monotonically decreasing. Therefore, a longer window length $L = 20$ is also used for the same simulated data set. Figure 3 shows that the NEES is not inconsistent in the beginning, for both the CMEKF and the Retrodicted CMEKF. The initial inconsistency is due to one point initialization [11]. When two points are used for initialization, the NEES is shown to be consistent from the beginning [12].

Figures 4 and 5 show that the RMSE in position and velocity obtained in the simulations for each algorithm, where $L = 20$. It is noted that the performance of the Retrodicted CMEKF is significantly better again. Most importantly, the error reduction becomes flat, which means future data beyond 10 frames does not significantly reduce the current RSMSE in position and velocity. Figure 6 shows the normalized estimation error squared (NEES) metric for this simulations. It shows both algorithms provided consistent state estimation for longer retrodiction length as well.

VI. CONCLUSIONS

A track retrodiction technique is investigated when the track output can be delayed. Monte Carlo simulation based on real radar parameters was used to evaluate the two algorithms: the CMEKF and the Retrodicted CMEKF. The simulation results show significant improvement in both the position and velocity errors, measured by RMSE. With a retrodiction length $L = 7$, the errors in position and velocity are reduced by 30% and by 25%, respectively. It is also observed that the error reduction is nonlinear with the number of retrodiction length and the retrodicted RMSE becomes flat when the length is over 10, which means future data beyond 10 frames does not help much to improve the current track accuracies. The NEES is used to check the error consistency. Both the CMEKF and the Retrodicted CMEKF are found to perform consistently. The

association retrodiction is only described briefly in the paper, which is recommended as a future topic.

REFERENCES

- [1] Ponsford, A.M., D'Souza, I.A. and Kirubarajan, T. (2009), Surveillance of the 200 nautical mile EEZ using HFSSWR in association with a spaced-based AIS interceptor, *Proc. of Technologies for Homeland Security*, pp. 87–92.
- [2] Drummond, O.E. (1993), Multiple target tracking with multiple frame, probabilistic data association, In O.E., Drummond, (Ed.), *Proc. of SPIE, on Signal and Data Processing of Small Targets*, Vol. 1954, pp. 394–408.
- [3] Drummond, O.E. (1995), Multiple sensor tracking with multiple frame, probabilistic data association, In O.E., Drummond, (Ed.), *Proc. of SPIE, on Signal and Data Processing of Small Targets*, Vol. 2561, pp. 322–336.
- [4] Drummond, O.E. (1997), Target tracking with retrodicted discrete probabilities, In O.E., Drummond, (Ed.), *Proc. of SPIE, on Signal and Data Processing of Small Targets*, Vol. 3163, pp. 249–268.
- [5] Bar-Shalom, Y. (2002), Update with out-of-sequence measurements in tracking: exact solution, *IEEE Transactions on Aerospace and Electronic Systems*, 38(3), 769–778.
- [6] Bar-Shalom, Y. and Chen, H. (2009), Removal of out-of-sequence measurements from tracks, *IEEE Transactions on Aerospace and Electronic Systems*, 45(2), 612–619.
- [7] Koch, W. (1996), Retrodiction for Bayesian multiple hypothesis/multiple target tracking in densely cluttered environment, In O.E., Drummond, (Ed.), *Proc. of SPIE, on Signal and Data Processing of Small Targets*, Vol. 2759, pp. 429–440.
- [8] Koch, W. (2000), Fixed-interval retrodiction approach to Bayesian IMM-MHT for maneuvering multiple targets, *IEEE Transactions on Aerospace and Electronic Systems*, 36(1), 2–14.
- [9] Poore, A., Lu, S. and Suchomel, B.J. (2009), Data association using multiple-frame assignments, 2 ed, Ch. 13, *Handbook of Multisensor Data Fusion*, pp. 299–318, CRC Press.
- [10] Rauch, H.E., Tung, F. and Striebel, C.T. (1965), Maximum likelihood estimates of linear dynamic systems, *AIAA Journal*, 3(8), 1445–1450.
- [11] Yeom, S.W., Kiruba, T. and Bar-Shalom, Y. (2004), Track segment association, fine-step IMM and initialization with Doppler for improved track performance, *IEEE Transactions of Aerospace and Electronic Systems*, 40, 239–309.
- [12] Ding, Z. and Balaji, B. (2010), Performance evaluation of four nonlinear filters for two radar applications, (DRDC Ottawa TM 2010-246) Defence R& D Canada - Ottawa.

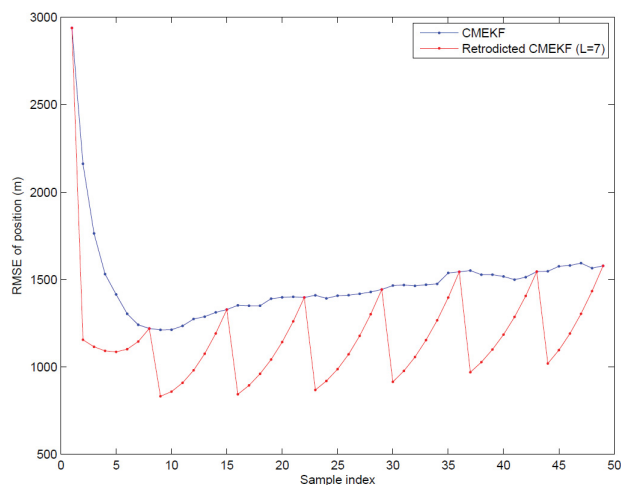


Fig. 1. RMSE in position when L=7.

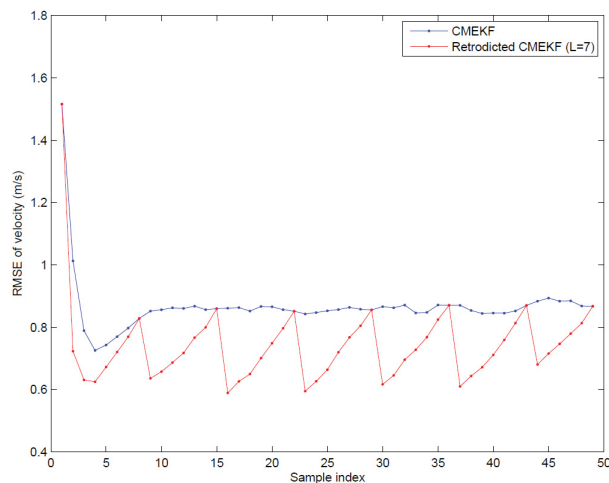


Fig. 2. RMSE in velocity when L=7.

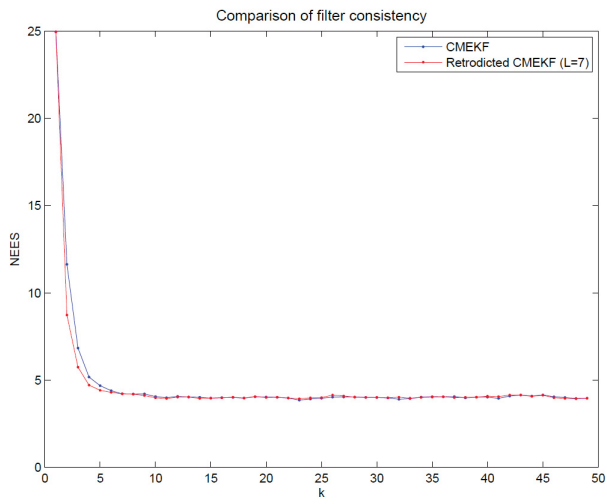


Fig. 3. NEES in simulations when $L=7$.

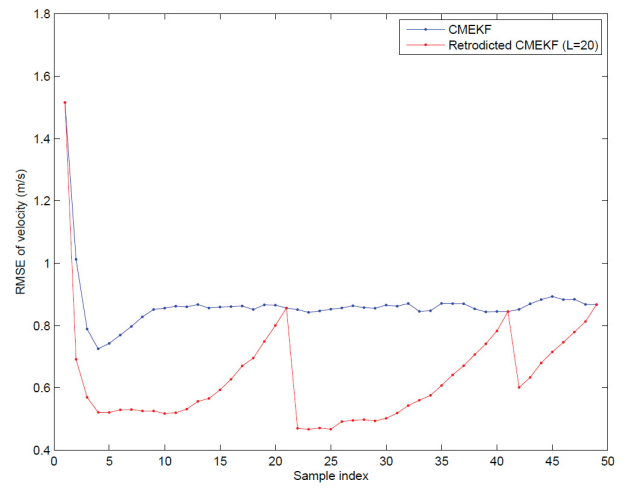


Fig. 5. RMSE in velocity when $L=20$.

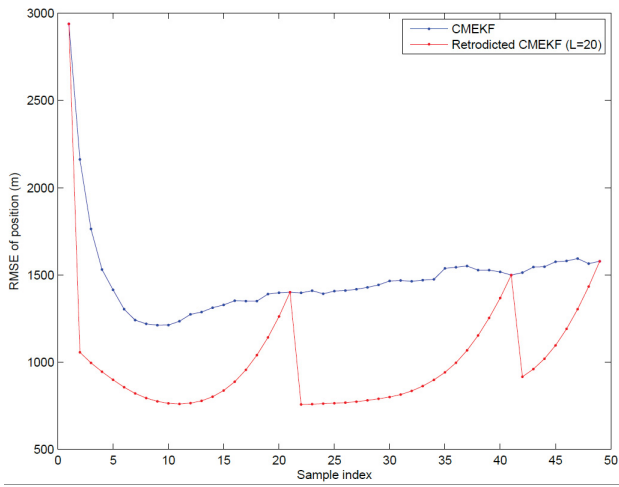


Fig. 4. RMSE in position when $L=20$.

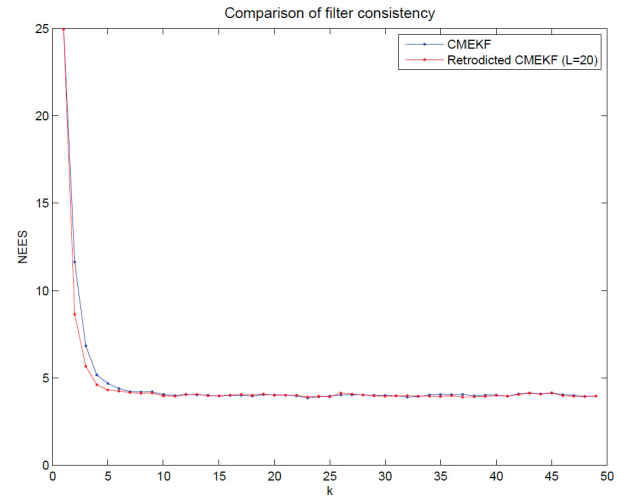


Fig. 6. NEES in simulations when $L=20$.